Nanocrystalline Material
(FINEMET)
datasheet

Nanocrystalline materials are emerging soft magnetic materials that possess grain sizes on the order of a billionth of a meter and possess extremely useful magnetic properties. These materials fill the gap between amorphous materials (without any long-range order) and conventional (coarse-grained) materials. Nanocrystalline alloys are materials on the basis of Fe (iron), Si (silicon), and B (boron), with additions of Nb (niobium) and Cu (copper). Typically, they are produced through a rapid solidification process as a thin, ductile ribbon. Initially the ribbon is in the amorphous state, then crystallized in a subsequent heat treatment to promote nano-crystallization (~10-20 nanometers). Once nano-crystallized, they exhibit low core loss and magnetostriction, while maintaining high saturation induction and permeability. A variety of forms can be manufactured, including toroidal, rectangular, racetrack, and block cores.

Date: September 2023
Revision 0.2

Fig. 1: Core under test (Nano-crystalline core).

Nano-crystalline core

Dimensions

Table 1: Core dimensions

Description	Symbol	Finished dimension (mm)
Width of core	A	180
Height of core	B	240
Depth of core (or cast width)	D	30
Thickness or build	E	50
Width of core window	F	80
Height of core window	G	140

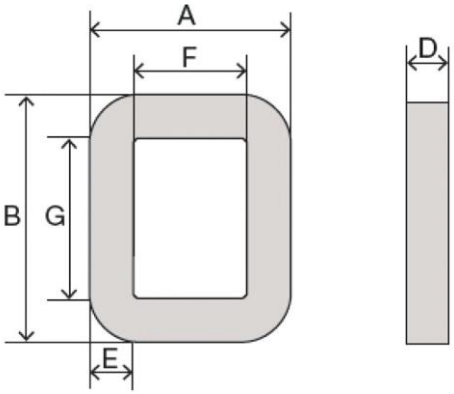

Fig. 2: Illustration of core dimensions.

Acknowledgement

This technical effort was performed in support of the National Energy Technology Laboratory's ongoing research in DOE's The Office of Electricity's (OE) Transformer Resilience and Advanced Components (TRAC) program.

NATIONAL ENERGY TECHNOLOGY LABORATORY

Magnetic Characteristics

Table 2: Magnetic characteristics

Description	Symbol	Typical value	Unit
Effective area	A_e	1,170	mm^2
Mean magnetic path length[1]	L_m	583	mm
Mass (before impregnation)		5.234	kg
Mass (after impregnation)		5.528	kg
Lamination thickness		0.0007 (0.0178)	inch (mm)
Chemistry		$Fe_{73.5}Nb_3Si_{15.5}B_7Cu_1$	
Grade		Nano-crystalline	
Anneal		Field Anneal	
Impregnation		100% Solids Epoxy	
Supplier		MK Magnetics	
Part number		4216MDT-B	

Measurement Setup

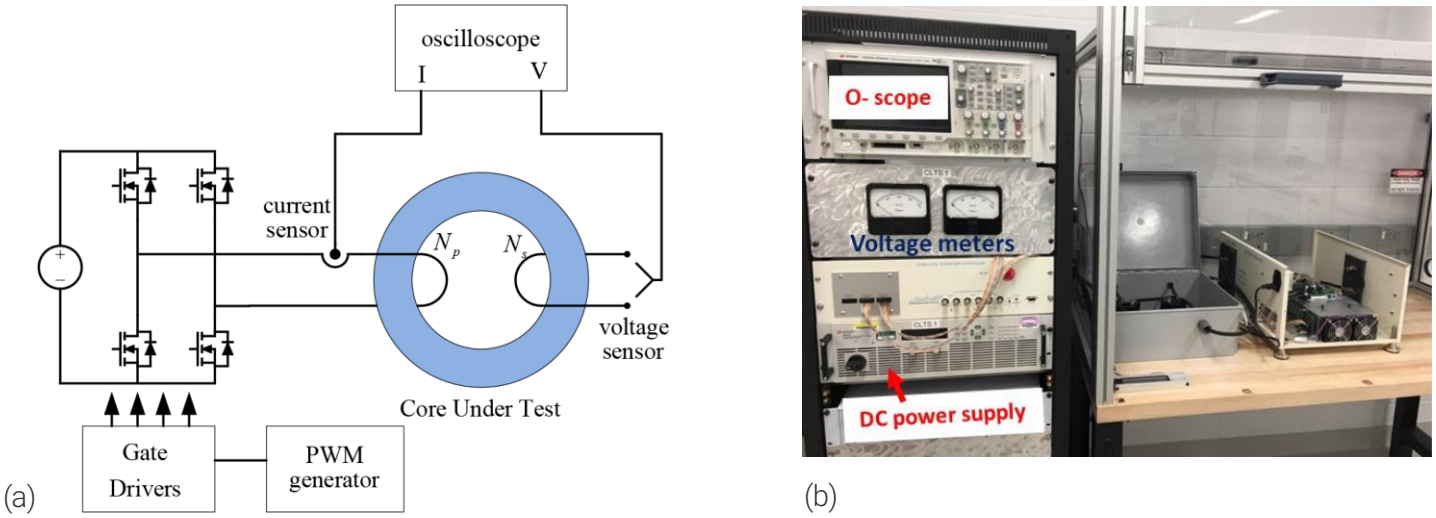

Fig. 3: Square waveform core loss test system (CLTS): (a) conceptual setup, (b) actual setup.

The *BH* curves, core losses, and permeability of the core under test (CUT) are measured with the square waveform core loss test system (CLTS), which is shown in Fig. 3. The square waveform CLTS is utilized to perform various square waveform measurements with different duty cycles, as shown in Fig. 4 (a) and (b). 1200V SiC MOSFET devices are utilized to extend the core characterization range.

[1] Mean magnetic path length is computed using the following equation. OD and ID are outer and inner diameters, respectively. $L_m = \frac{\pi(\mathrm{OD}-\mathrm{ID})}{\ln\left(\frac{\mathrm{OD}}{\mathrm{ID}}\right)}$

Two windings are placed around the core under test. The output waveform excites the primary winding, and the current of the primary winding is measured, in which the current information is converted to the magnetic field strengths *H* as

$$H(t) = \frac{N_p \cdot i(t)}{l_m}, \tag{1}$$

where N_p is the number of turns in the primary winding. A dc-biasing capacitor is inserted in the series with the primary winding to provide zero average voltage applied to the primary winding.

The secondary winding is open, and the voltage across the secondary winding is measured, in which the voltage information is integrated to derive the flux density B as

$$B(t) = \frac{1}{N_s \cdot A_e} \int_0^T v(\tau)\, d\tau, \tag{2}$$

where N_s is the number of turns in the secondary winding, and T is the period of the excitation waveform.

Fig. 4 illustrates two different excitation voltage waveforms and corresponding flux density waveforms. When the excitation voltage is a two-level square waveform as shown in Fig. 4(a), the flux is a sawtooth shape. The average excitation voltage is adjusted to be zero via the dc-biasing capacitor, and thus, the average flux is also zero. When the excitation voltage is a three-level square voltage as shown in Fig. 4(b), the flux is a trapezoidal shape. The duty cycle is defined as the ratio between the applied high voltage time and the period. In the sawtooth flux, the duty cycle can range from 0% to 100%. In the trapezoidal flux, the duty cycle range from 10% to 50%. At 50% duty cycles, both the sawtooth and trapezoidal waveforms become identical.

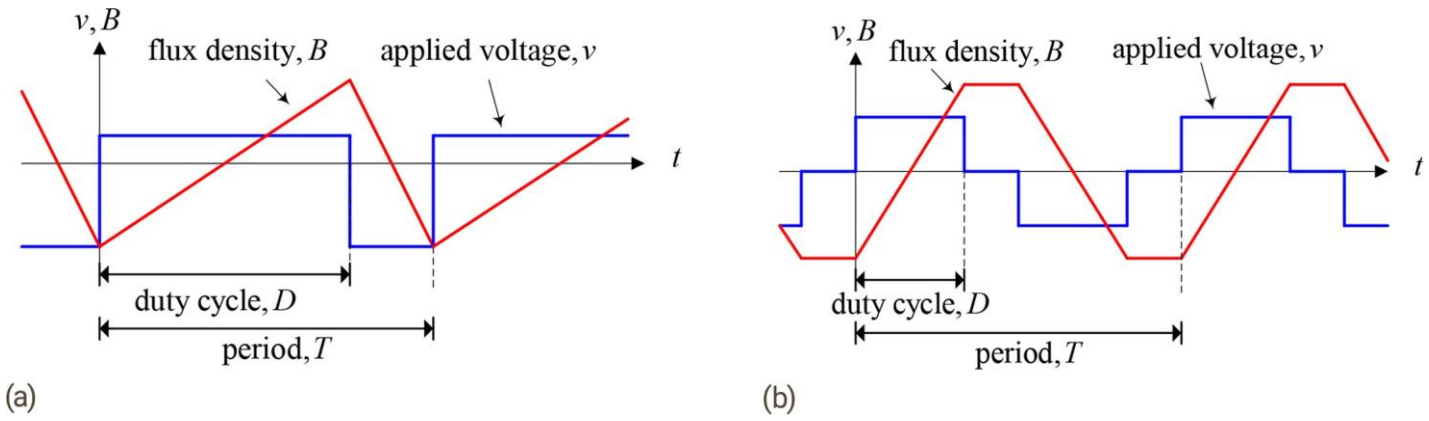

Fig. 4: Excitation voltage waveforms and corresponding flux density waveforms: (a) Sawtooth flux, and (b) trapezoidal flux.

Anhysteritic BH Curves

Fig. 5 illustrates the measured low frequency *BH* loops at 500 Hz. Using the *BH* loop, the anhysteretic *BH* curve is fitted. The anhysteretic *BH* curves can be computed as a function of field intensity *H* using the following formula.

$$B = \mu_H(H)H$$

$$\mu_H(H) = \mu_0 + \sum_{k=1}^{K} \frac{m_k}{h_k \left(1 + \left|H/h_k\right|^{n_k}\right)} \tag{3}$$

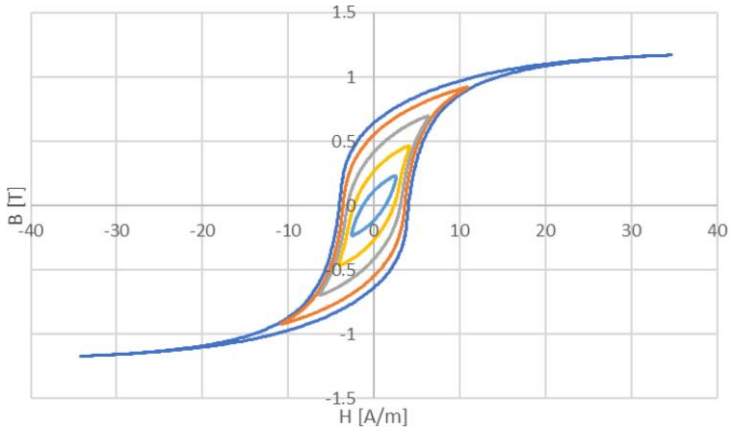

Fig. 5: Low frequency BH loops (excitation at 500 Hz).

Similarly, the anhysteretic *BH* curves can be computed as a function of flux density *B* using the following formula.

$$B = \mu_B(B)H$$

$$\mu_B(B) = \mu_0 \frac{r(B)}{r(B) - 1}$$

$$r(B) = \frac{\mu}{\mu_r - 1} + \sum_{k=1}^{K} \alpha_k |B| + \delta_k \ln\left(\varepsilon_k + \zeta_k e^{-\beta_k |B|}\right) \tag{4}$$

$$\delta_k = \frac{\alpha_k}{\beta_k}, \varepsilon_k = \frac{e^{-\beta_k \gamma_k}}{1 + e^{-\beta_k \gamma_k}}, \zeta_k = \frac{1}{1 + e^{-\beta_k \gamma_k}}$$

Table 3 and Table 4 list the anhysteretic curve coefficients for eqs. (3) and (4), respectively.

The core anhysteretic characteristic models in eqs. (3) and (4) are based on the following references.

Scott D. Sudhoff, "Magnetics and Magnetic Equivalent Circuits," in *Power Magnetic Devices: A Multi-Objective Design Approach*, 1, Wiley-IEEE Press, 2014, pp.488-

G. M. Shane and S. D. Sudhoff, "Refinements in Anhysteretic Characterization and Permeability Modeling," in *IEEE Transactions on Magnetics*, vol. 46, no. 11, pp. 3834-3843, Nov. 2010.

The estimation of the anhysteretic characteristic is performed using a genetic optimization program, which can be found in the following websites:

https://engineering.purdue.edu/ECE/Research/Areas/PEDS/go_system_engineering_toolbox

Table 3: Anhysteretic curve coefficients for B as a function of H

k	1	2	3	4
m_k	1.45432290901190	-0.787469528017856	0.305816513846983	-0.100099666071160
h_k	1.66901849037468	4.53941231474504	16.3984489615004	2.21434113438350
n_k	1	1.39181845814425	1.91929608345426	2.47225983230501

Table 4: Anhysteretic curve coefficients for H as a function of B

k	1	2	3	4
μ_r	122403.680741993			
α_k	0.601590372006389	0.0373154057929699	0.0371340984781102	0.00547195463929012
β_k	49.0941919818141	6.05165057248446	342.771453167956	26.7566654427740
γ_k	1.43228670933891	2.10625323925708	1.41322170444317	1.30002822552914
δ_k	0.0122537992320810	0.00616615340658217	0.000108334863171685	0.000204508093543767
ε_k	2.89556194654586e-31	2.91304528523862e-06	4.19291980155985e-211	7.82200715654711e-16
ζ_k	1	0.999997086954715	1	0.999999999999999

Fig. 6 illustrates the measured *BH* curve and fitted anhysteretic *BH* curves as functions of *H* and *B* using the coefficients from Table 3 and Table 4. Fig. 7 and Fig. 8 illustrate the absolute relative permeability as functions of field strength *H* and flux density *B*, respectively. Fig. 9 illustrates the incremental relative permeability.

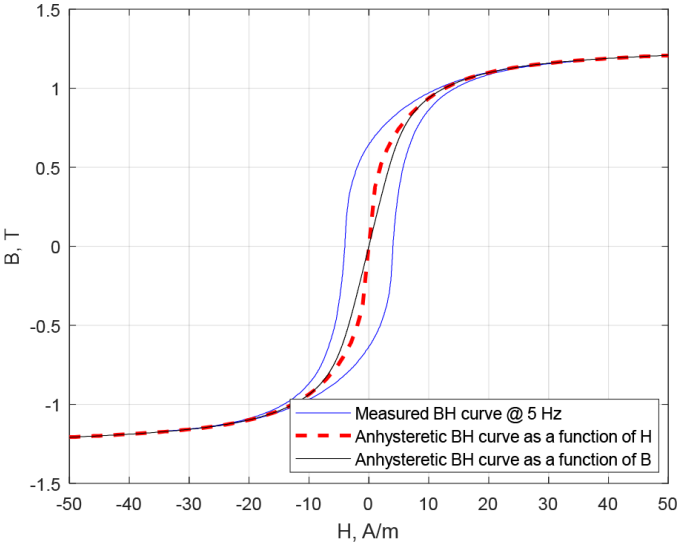

Fig. 6: Measured BH curve and fitted anhysteretic BH curve as functions of H and B.

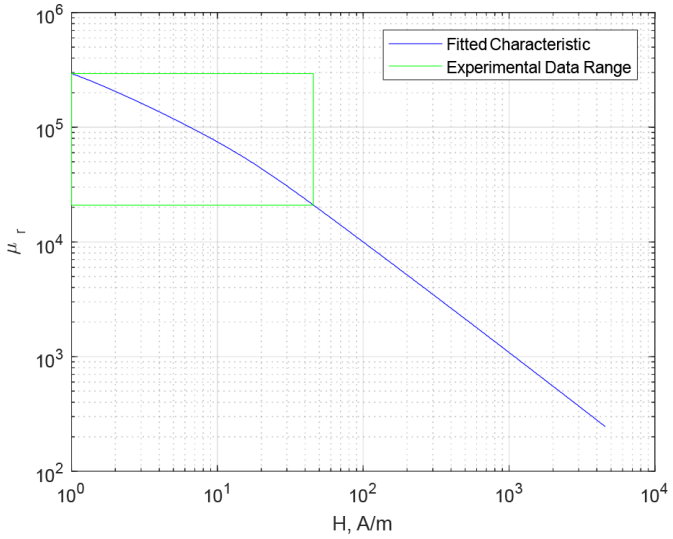

Fig. 7: Absolute relative permeability as function of field strength H.

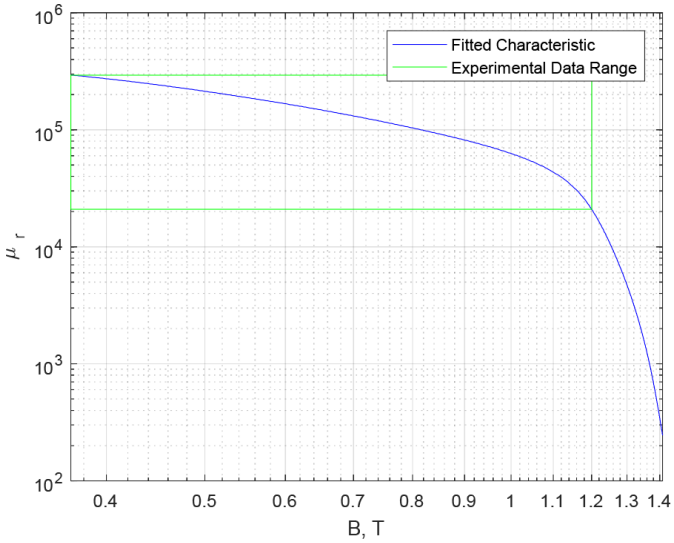

Fig. 8: Absolute relative permeability as function of flux density B.

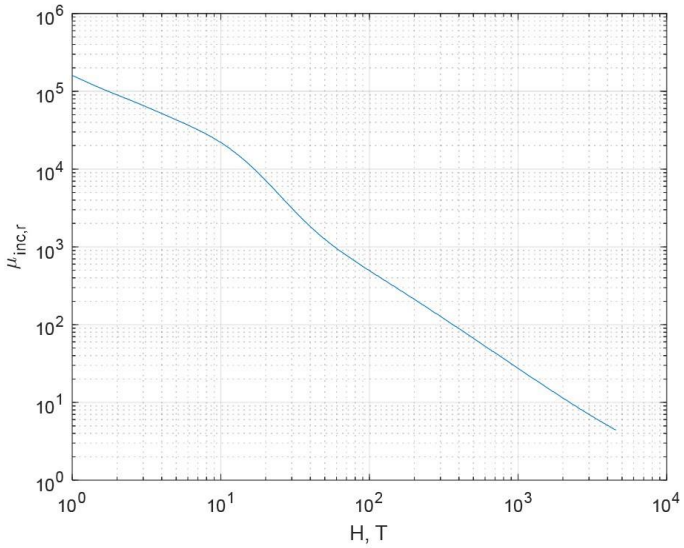

Fig. 9: Incremental relative permeability.

Core Losses

Core losses at various frequencies and induction levels are measured using various excitation waveforms. Based on measurements, the coefficients of the Steinmetz's equation are estimated. The Steinmetz's equation is given as

$$P_w = k_w \cdot (f / f_0)^{\alpha} \cdot (B / B_0)^{\beta} \tag{5}$$

where P_w is the core loss per unit weight, f_0 is the base frequency, B_0 is the base flux density, and k_w, α, and β are the Steinmetz coefficients from empirical data. In the computation of P_w, the weight before impregnation in Table 2 is used, the base frequency f_0 is 1 Hz, and the base flux density B_0 is 1 Tesla.

Fig. 10 illustrates the measured *BH* curve at different frequencies. The field strength *H* is kept near constant for all frequency. At 5 kHz and 10 kHz excitations, the *BH* curve is similar, which indicates that the hysteretic losses are the dominant factor at frequencies below 10 kHz. As frequency increases, the *BH* curves become thicker, which indicates that the eddy current and anomalous losses are becoming larger.

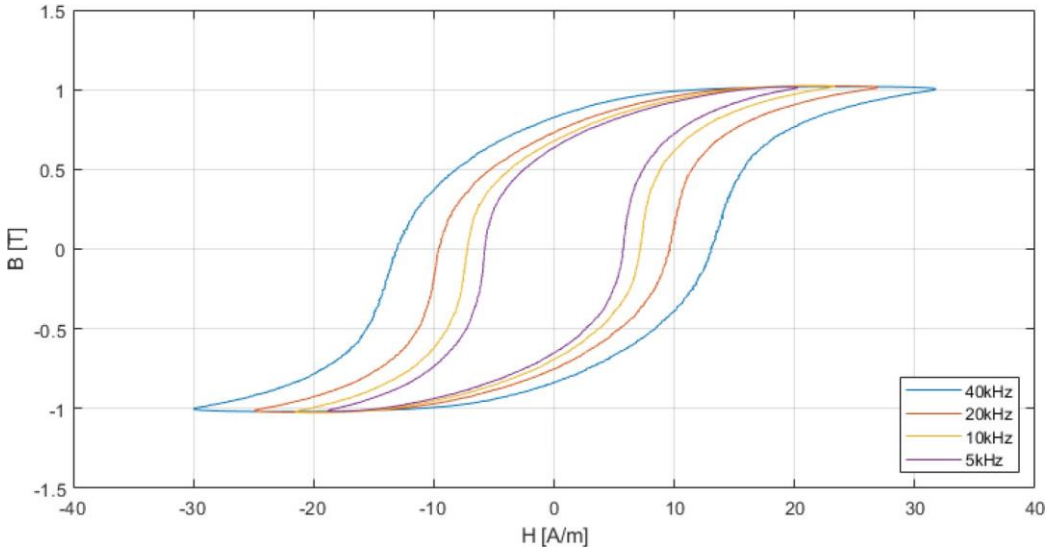

Fig. 10: BH curve as a function of frequency.

Table 5 lists the Steinmetz coefficients at different excitation conditions, and Fig. 11 and Fig. 12 illustrate the core loss measurements and estimations via Steinmetz equation.

Table 5: Steinmetz coefficients

	k_w	α	β
Sawtooth/Trapezoidal 50% duty	0.0000269090	1.5055	2.0467
Trapezoidal 40% duty	0.0000186090	1.5586	2.0114
Trapezoidal 30% duty	0.0000171360	1.585	1.9543
Trapezoidal 20% duty	0.0000126660	1.6427	1.9274
Trapezoidal 10% duty	0.0000078330	1.7392	1.8827
Sawtooth 40% duty	0.0000064772	1.6595	2.2601
Sawtooth 30% duty	0.0000105120	1.6224	2.1081
Sawtooth 20% duty	0.0000053969	1.7085	2.1265
Sawtooth 10% duty	0.0000034059	1.8114	2.066

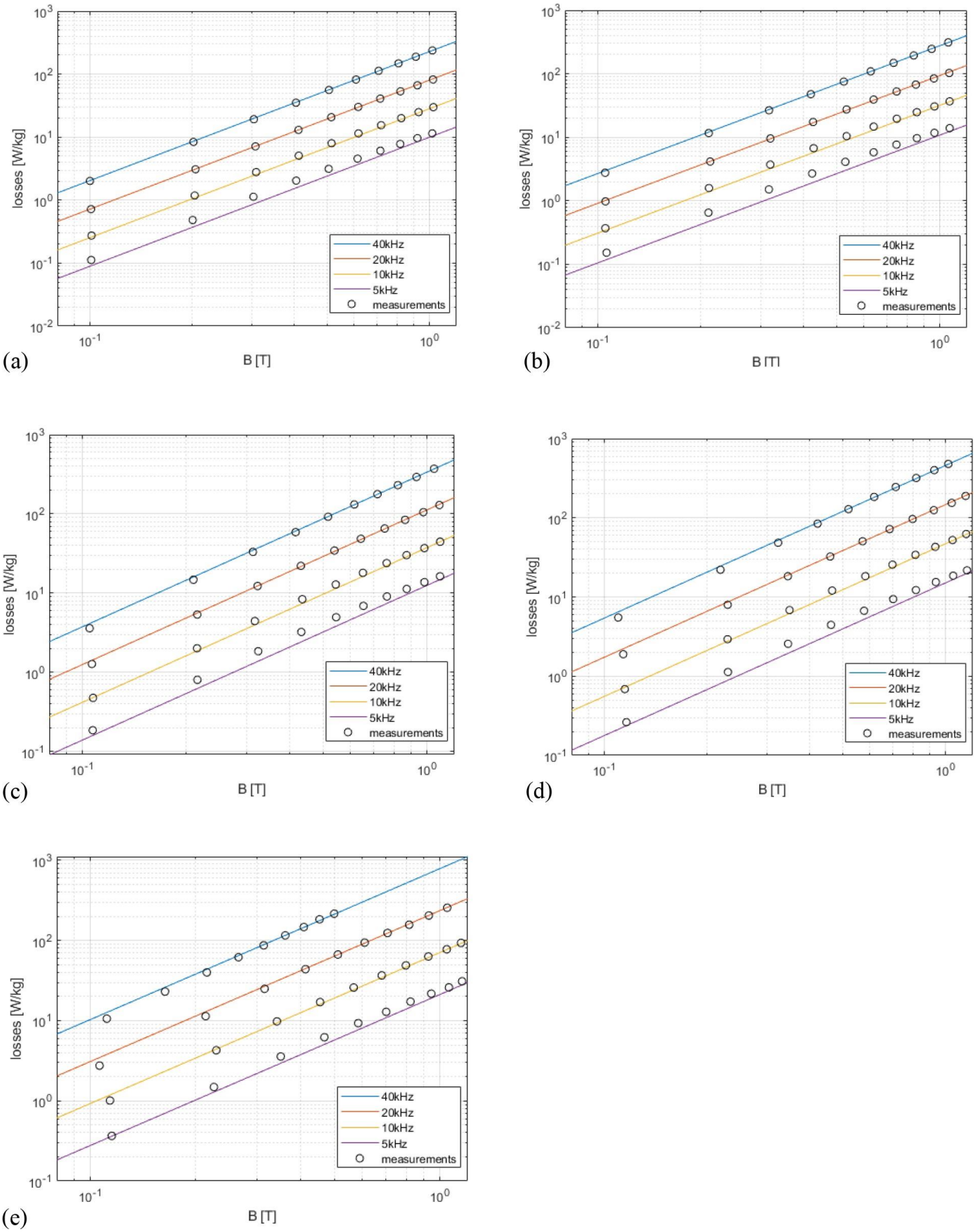

Fig. 11: Core loss measurements and estimations via Steinmetz equation: (a) Sawtooth/Trapezoidal 50% duty, (b) Trapezoidal 40% duty, (c) Trapezoidal 30% duty, (d) Trapezoidal 20% duty, and (e) Trapezoidal 10% duty.

Core Permeability

The permeability of the core is measured as a function of flux density and frequency. Fig. 13 and Fig. 14 illustrate the measured absolute relative permeability μ_r values, which is defined as

$$\mu_r = \frac{B_{peak}}{\mu_0 \cdot H_{peak}} \tag{6}$$

where B_{peak} and H_{peak} are the maximum flux density and field strength at each measurement point. Under certain excitation conditions, the core could not be saturated due to lack of available voltages. For example, the square CLTS could not saturate the core during the highest frequency and 10% duty cycle.

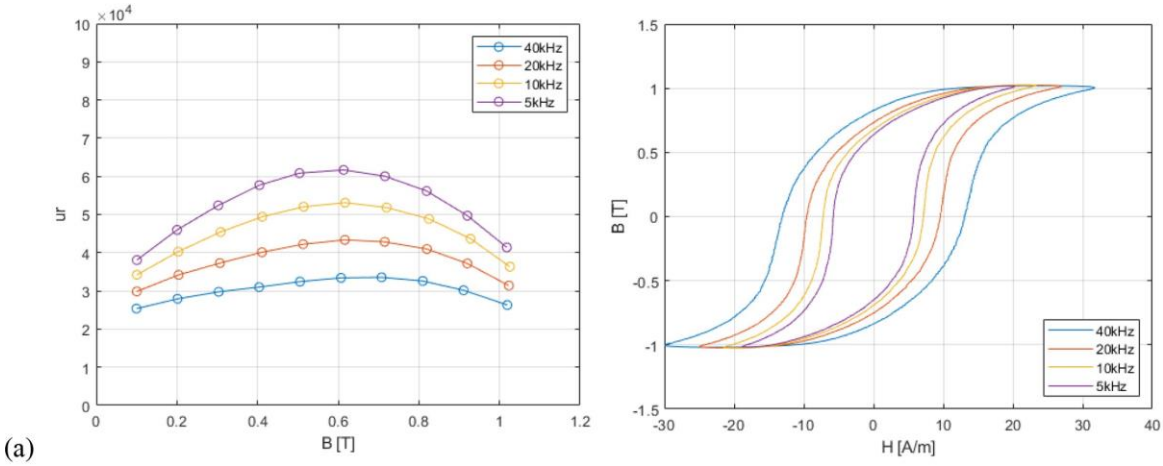

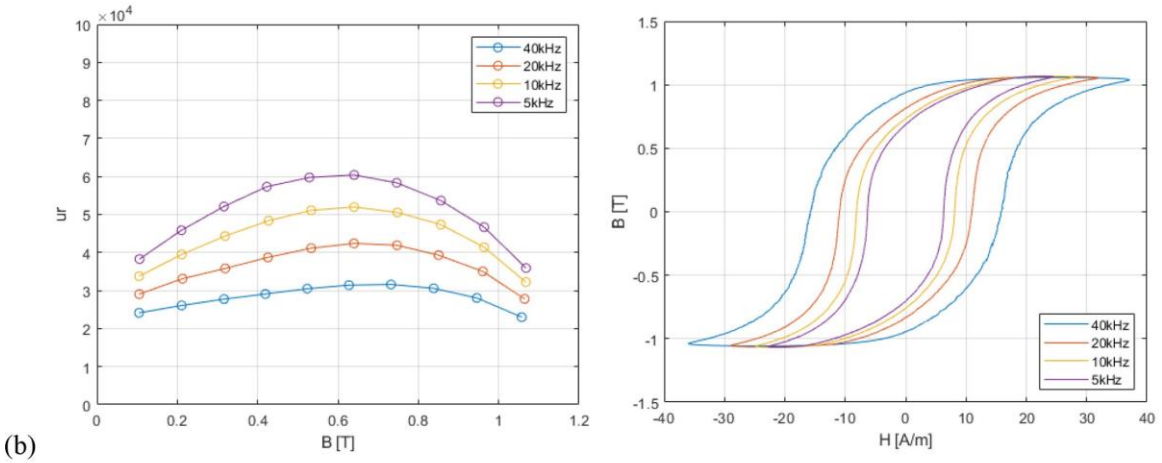

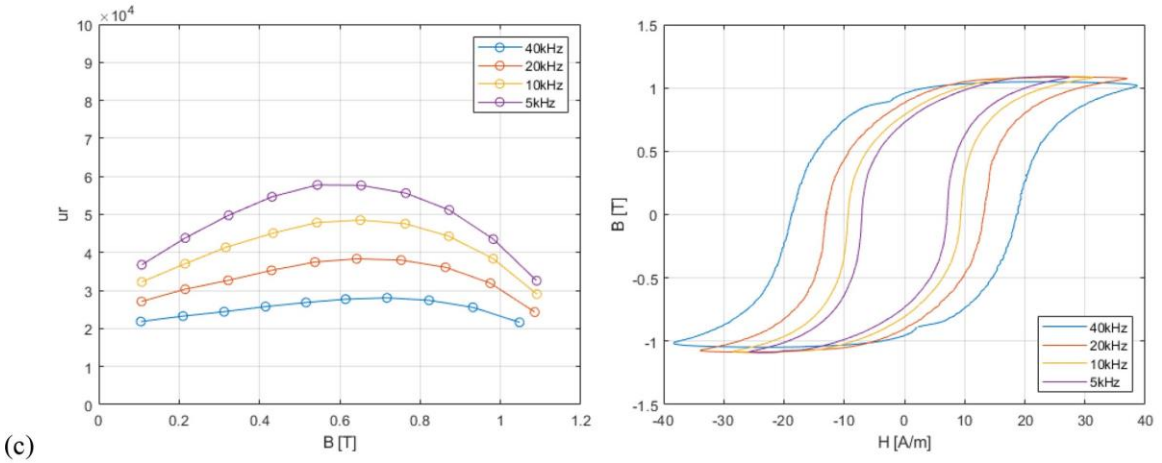

(continued on page 9

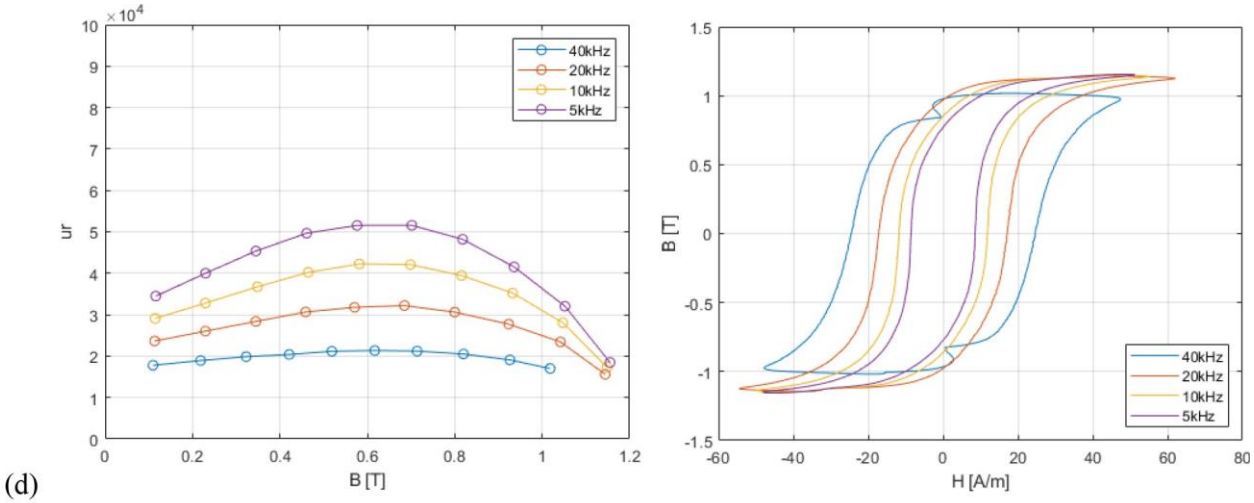

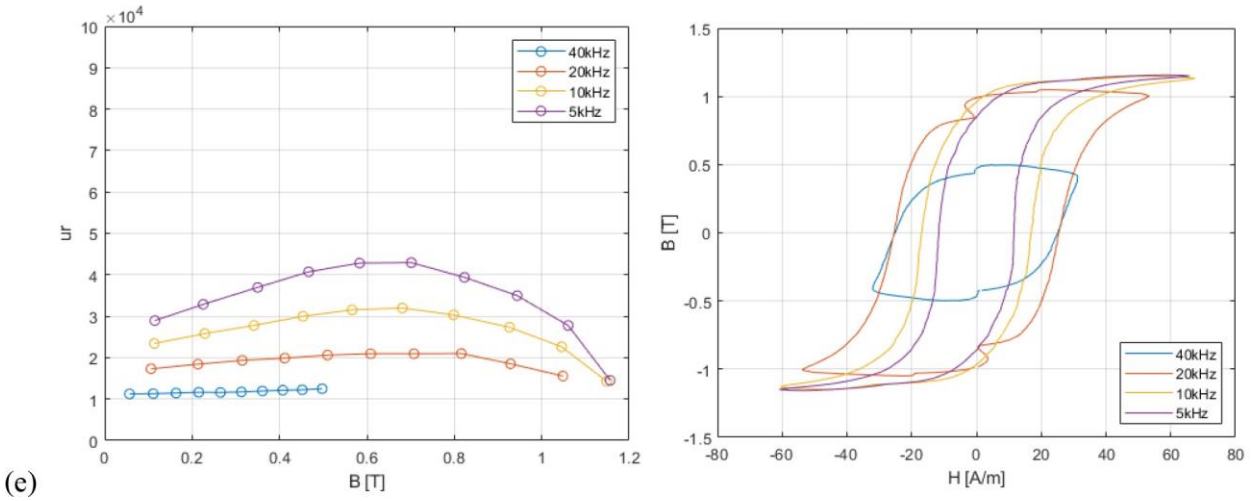

Fig. 13 Symmetrical excitation with various duty cycle: relative permeability as a function of flux density and frequency (left column) and BH loop at the maximum B of the corresponding frequency (right column): (a) 50% duty, (b) 40% duty, (c) 30% duty, (d) 20% duty, and (e) 10% duty (could not saturate the core under the condition).*

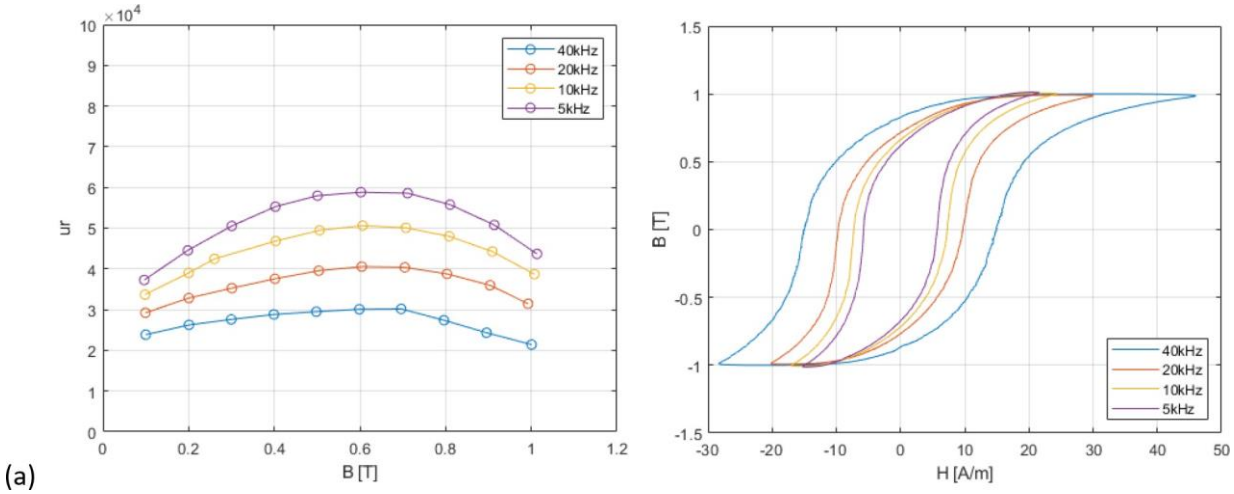

(continued on page 10)

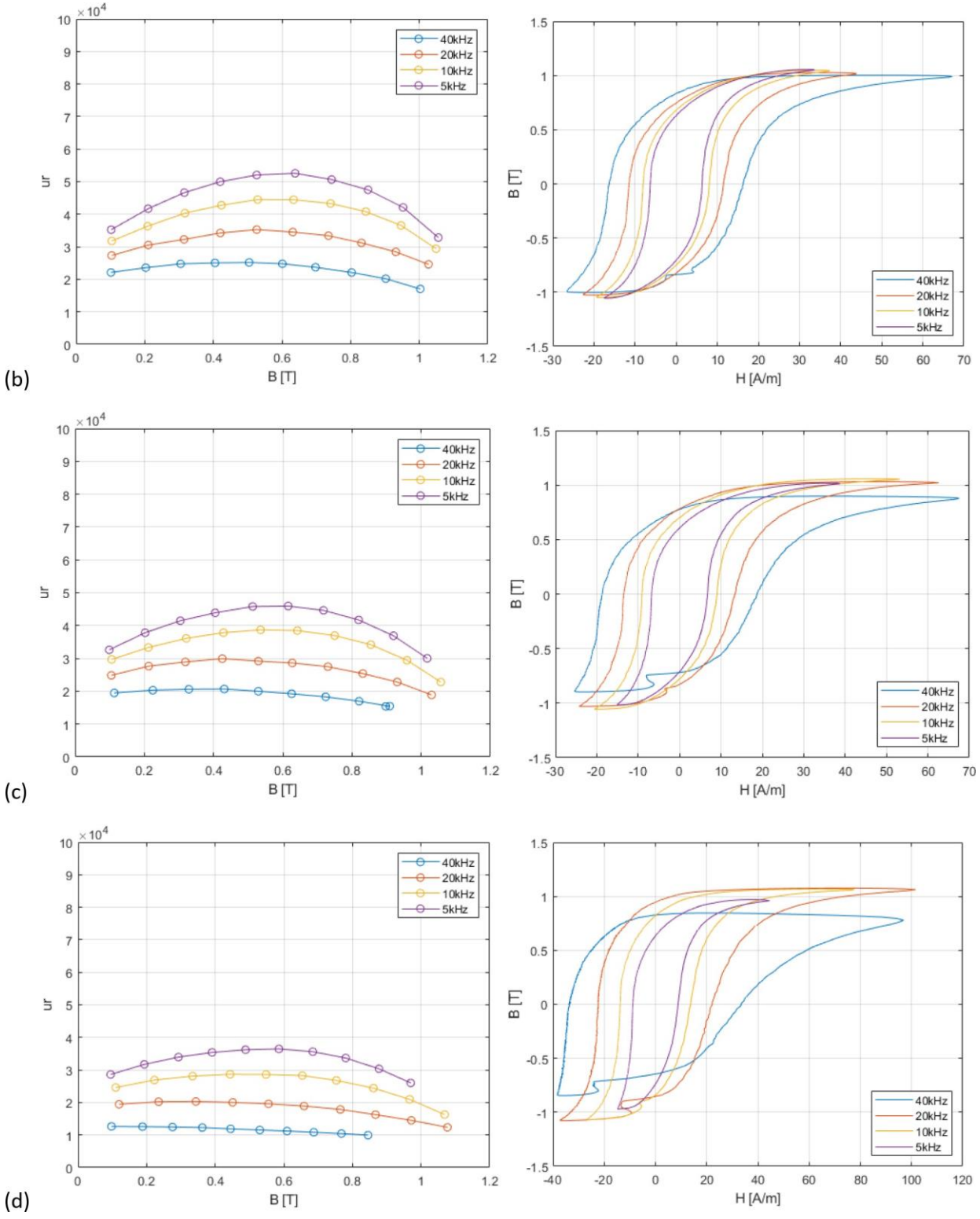

Fig. 14 Asymmetrical excitation with various duty cycle: relative permeability as a function of flux density and frequency (left column) and BH loop at the maximum B of the corresponding frequency (right column): (a) 40% duty, (b) 30% duty, (c) 20% duty, and (d) 10% duty.